

## A New Generalization of the Standard Electrokinetic Model

J. J. López-García,<sup>†</sup> C. Grosse,<sup>‡,§</sup> and J. Horno<sup>\*,†</sup>

*Departamento de Física, Universidad de Jaén, Campus Las Lagunillas, Ed. A-3, 23071, Jaén, Spain,  
Departamento de Física, Universidad Nacional de Tucumán, Av. Independencia 1800, 4000 San Miguel de  
Tucumán, Argentina, and Consejo Nacional de Investigaciones Científicas y Técnicas, Argentina*

*Received: February 26, 2007; In Final Form: May 11, 2007*

We present a new generalization of the standard electrokinetic model based on the assumption that there is a thin layer surrounding the suspended particle where the equilibrium ion density is not determined by the Gouy–Chapman distribution, while the standard model applies outside this layer. Our approach differs from existing models in that we consider that the surface layer is made both of free ions (mostly counterions) and of the fixed ions that constitute the charge of the particle. Furthermore, the free ion density is determined by appropriate boundary conditions without considering any adsorption isotherms. Finally, the fluid is allowed to freely flow inside the layer, only hindered by the presence of the fixed charges and the adhesion condition on the surface of the particle. We show that this generalization leads to results that qualitatively differ from those obtained using existing models: instead of always decreasing, the electrophoretic mobility can actually increase with the anomalous surface conductivity. This could make it possible to use our model for the interpretation of a broader set of experimental data, including those cases when the measured mobility is higher than predicted by the standard model.

### 1. Introduction

According to the classical description of colloidal suspensions, the main parameter determining their dielectric and electrokinetic properties is the  $\zeta$  potential. This parameter is determined experimentally by means of electrophoretic mobility measurements and using the so-called standard electrokinetic model. According to this model, the particles are surrounded by a uniform surface density of fixed charge, the ions in the electrolyte solution can be treated as mathematical points, and macroscopic values of the permittivity and viscosity remain valid at the microscopic scale up to the very surface of the particle. Under these assumptions, the equilibrium distribution of ions around a suspended particle coincides with the Gouy–Chapman distribution, the  $\zeta$  potential coincides with the equilibrium electric potential at its surface, and the surface conductivity coincides with the conductivity of its diffuse double layer.

Therefore, the surface conductivity value is a function of the  $\zeta$  potential and of other known parameters of the model such as the ion concentrations in the electrolyte solution far from the particle, their valences, diffusion coefficients, and the fluid viscosity. This means that all the dielectric and electrokinetic properties of the system should be functions of a series of known parameters and of a single variable: the  $\zeta$  potential. This result has been used for many decades to determine  $\zeta$  by means of a single measurement: the electrophoretic mobility. An equally valid alternative is to determine its value from the conductivity increment, since both phenomena are described by means of the same standard model. The problem that arises is that, quite often, the  $\zeta$  potential values obtained using these two techniques do not coincide with one another.<sup>1–3</sup>

While the reason for this discrepancy is not known, it seems that its origin is in a fundamental failure of the standard

electrokinetic model: the surface of a colloidal particle appears to be more complex than assumed by this model. An often used generalization is based on the Stern rather than the Gouy–Chapman distribution of ions around the particle. It is assumed that the particle surface bearing the fixed charge density is surrounded by a thin layer of ions (mostly counterions), with a surface density determined by adsorption isotherms rather than the Poisson–Boltzmann equation.<sup>4–6</sup> Outside this layer, the system satisfies the Gouy–Chapman distribution. Out of equilibrium, the properties of this generalized model are determined by assuming that the liquid in the thin ion layer is not allowed to move, while the ions are free to move along the surface with a mobility that is comparable to that in the bulk solution. Because of this assumption, the  $\zeta$  potential coincides now with the equilibrium electric potential at the outer surface of the thin ion layer, rather than the particle surface.

This generalization implies that the surface conductivity of the particle is now made of two terms: the diffuse double layer part determined by the standard model, and the conductivity of the inner layer of ions determined by adsorption. Therefore, the surface properties depend now on two parameters: the  $\zeta$  potential and the surface conductivity of the inner layer, also known as the anomalous surface conductivity. In view of this dependence, it is no longer possible to determine the  $\zeta$  potential from a single measurement such as the electrophoretic mobility or conductivity increment. Both measurements are required.

While this appears to solve the compatibility problem between the  $\zeta$  potential values deduced from these two individual measurements,<sup>7</sup> a serious problem remains: the presence of the anomalous surface conductivity always decreases the electrophoretic mobility value. Therefore, this generalization of the standard model does not help and actually worsens the interpretation in those cases when the measured electrophoretic mobility is very high, higher than the theoretical maximum.<sup>8</sup> Still another difficulty arises when the models are extended into

<sup>†</sup> Universidad de Jaén.

<sup>‡</sup> Universidad Nacional de Tucumán.

<sup>§</sup> Consejo Nacional de Investigaciones Científicas y Técnicas.

the frequency domain<sup>9–11</sup> and the low-frequency dielectric dispersion predictions are compared with experimental data.<sup>12–14</sup> It is observed that the measured dispersion amplitude can be much higher than the theoretical prediction, while the characteristic frequency is much lower. In many cases, no combination of model parameters can explain the measured permittivity values, even when the static mobility and conductivity data can be interpreted.

An interesting example of this situation is presented in refs 15 and 16, where it is shown that after a heating treatment the latex particles behave almost ideally. This suggests that, in its original state, polystyrene particles can have a hairy rather than a flat surface. Actually, this assumption was previously used as another type of generalization of the standard model. Instead of considering that the particle surface is perfectly flat and rigid, it was modeled as a hairy surface<sup>17,18</sup> or as a thin porous layer.<sup>19</sup>

Still another generalization of the standard model consists of taking into account the tiny concentrations of H<sup>+</sup> and OH<sup>-</sup> ions, always present in aqueous electrolyte solutions, in addition to the relatively large concentrations of, for example, Cl<sup>-</sup> and K<sup>+</sup> ions that are usually the only ions considered when the standard model is used. The inclusion of these additional ions is formally straightforward, even when it represents a tremendous complication in the calculations. However, if treated just as the remaining ions, their influence on the dielectric and electrokinetic properties would remain negligible, despite their high mobility, in view of their low concentration. But there is good reason to believe that these ions should be treated differently: the  $\zeta$  potential of suspended particles usually depends on the pH value of the suspending medium. This observation led to different generalizations of the standard model in which H<sup>+</sup> and OH<sup>-</sup> ions are allowed to adsorb to the surface of the particle, changing the local value of its formally fixed surface charge.<sup>10,11,20,21</sup>

In this work, we present a new generalization of the standard electrokinetic model that can be regarded as a modification of the first approach. It is also based on the assumption that there is a thin layer surrounding the particle where the ion density is not determined by the Gouy–Chapman distribution. Again, the standard model applies outside this layer. The difference with existing generalizations is limited, therefore, to the surface layer properties. We consider that it is made both of free ions (mostly counterions) and of the fixed ions that constitute the surface charge. This makes it possible to model the surface layer as a thin charged polymer layer surrounding the particle, just as in the case of soft particles. This representation has two main consequences. First, there is a finite density of free ions inside the layer determined by appropriate boundary conditions, even without considering any adsorption isotherms. Second, it is no longer obvious that there is no fluid flow inside the surface layer. On the contrary, the fluid can be allowed to freely flow along the surface of the particle, only hindered by the presence of the fixed charges and this adhesion condition valid on its surface. We show that this generalization can lead to results that qualitatively differ from those obtained using the existing approach: instead of always decreasing, the electrophoretic mobility can actually increase with the anomalous surface conductivity. This fact extends the range of experimental data that can be interpreted by the model, including those cases where the measured mobility is higher than predicted by the standard model.

## 2. Model

### 2.1. Brief Review of the Mangelsdorf and White Model.

Before discussing in detail the proposed model, it is advisable

to review the main features of the model of Mangelsdorf and White (M–W),<sup>6,10</sup> which we will use for comparison. In that model, it is assumed that a suspended particle is surrounded by the Stern layer and that its “electrokinetic radius”  $a$  includes that layer, so that standard electrokinetic equations are valid for  $r > a$ . The outer boundary of the Stern layer is located at a distance  $x = \beta_1 + \beta_2$ , measured from the surface of the particle core. Therefore, in equilibrium, the Gouy–Chapman ion distribution applies for  $x > \beta_1 + \beta_2$  and the fixed surface charge density is located precisely at the core surface:  $x = 0$ . The adsorbed ions are assumed to lie adjacent to the surface, with their centers located at  $x = \beta_1$ , so that their charge can be represented by a surface charge density  $\sigma_s^0$ .

The surface charge density in the Stern layer is determined by means of an adsorption Langevin type isotherm

$$\sigma_{sj}^0 = z_j e N_j \frac{\frac{n_j^\infty}{K_j} \exp\left(\frac{-z_j e}{k_B T} \Psi^0(\beta_1)\right)}{1 + \sum_{k=1}^N \frac{n_k^\infty}{K_k} \exp\left(\frac{-z_k e}{k_B T} \Psi^0(\beta_1)\right)} \quad (1)$$

where the lower index  $j$  refers to the ion type,  $z_j e$  is the ion charge,  $n_j^\infty$  its bulk molar density,  $K_j$  the dissociation constant, and  $N_j$  the maximum surface density allowed at  $x = \beta_1$  for ions of type  $j$ . Finally,  $N$  is the number of ion types present in the solution,  $k_B$  represents the Boltzmann constant,  $T$  the absolute temperature, and  $\Psi^0 = \Psi^0(x)$  the equilibrium electric potential. Actually, two adsorption isotherms are considered: adsorption onto “underlying area”, eq 1, and adsorption onto “underlying charge”, expressed by an isotherm identical to eq 1, except that the summation over all the ion species in the denominator is replaced just by the  $j$  ion type term. However, numerical calculations are only made by considering the first kind of adsorption isotherm, so that we shall not consider the second case in what follows. In these calculations,  $N_j$  is deduced from the maximum surface charge density that is assigned the values:  $eN_j = 30$  or  $80 \mu\text{C cm}^{-2}$  while  $K_j$  (in mol/L) is expressed as  $K_j = 10^{-pK_j}$ , where  $pK_j$  is considered to be in the range from  $-1$  to  $2$ .

In view of the thinness of the Stern layer, the value of the potential at  $x = \beta_1$  is related to the corresponding value at  $x = \beta_1 + \beta_2$  using plane geometry

$$\Psi^0(\beta_1) = \zeta - \frac{\sigma_d^0}{C_2} \quad (2)$$

where  $\sigma_d^0$  is the surface charge of the diffuse double layer and  $C_2$  is the outer Stern layer capacity per unit area. Writing this capacity as

$$C_2 = \epsilon/\beta_2$$

and substituting  $C_2 = 130 \mu\text{F cm}^{-2}$ , used in ref 10 for all the numerical calculations, and  $\epsilon = 78.55 \times 8.85 \times 10^{-12} \text{ F m}^{-1}$ , leads to the value  $\beta_2 = 5.3 \times 10^{-10} \text{ m}$  (a different value of the permittivity in the Stern layer could certainly be considered, but this would require the incorporation of a Born-type energy term<sup>22</sup> in eq 1). Therefore, the thickness of the Stern layer considered in the M–W model is on the order of  $h \equiv \beta_1 + \beta_2 \approx 10 \times 10^{-10} \text{ m}$ . This value is not used in the calculations, since the layer is treated as if it were infinitely thin.

It is interesting to compare the total average volume density of ions inside the Stern layer

$$n_{\text{av}}^0 = \frac{1}{h} \sum_{j=1}^N \frac{\sigma_{sj}^0}{z_j e} \quad (3)$$

with the total ion density in the diffuse double layer at its boundary

$$n^0(a) = \sum_{j=1}^N n_j^0(a) = \sum_{j=1}^N n_j^\infty \exp\left(\frac{-z_j e \zeta}{k_B T}\right) \quad (4)$$

This can be done combining eqs 1 and 2

$$\sigma_{sj}^0 = n_j^0(a) \frac{\frac{z_j e N_j}{K_j} \exp\left(\frac{z_j e \sigma_d^0}{k_B T C_2}\right)}{1 + \sum_{k=1}^N \frac{n_k^\infty}{K_k} \exp\left(\frac{-z_k e \zeta}{k_B T}\right) \exp\left(\frac{z_k e \sigma_d^0}{k_B T C_2}\right)} \quad (5)$$

and using the following expression for the diffuse double layer surface charge density, which is valid for thin double layers and binary electrolytes with equal counterion and co-ion valences<sup>23</sup>

$$\sigma_d^0 = \frac{4e n^\infty 1000 N_A}{\kappa} \sinh\left(\frac{e \zeta}{2k_B T}\right) \quad (6)$$

where

$$\kappa = \sqrt{\frac{2e^2 n^\infty 1000 N_A}{\epsilon k_B T}} \quad (7)$$

is the reciprocal Debye length,  $N_A$  is the Avogadro number, and it was assumed that the electrolyte is univalent.

The obtained results for the total average ion density inside the Stern layer as a function of the equilibrium dimensionless surface potential

$$y^0(a) = \frac{e \Psi^0(a)}{k_B T}$$

calculated for  $a = 100$  nm particles in a binary univalent electrolyte solution such that  $\kappa a = 30$  and considering that  $eN_j = 80 \mu\text{C cm}^{-2}$  are presented in Figure 1. The same values represented as a function of  $\kappa a$  and calculated for  $y^0(a) = 4$  are presented in Figure 2. In this last figure, the surface charge of the diffuse layer was obtained numerically rather than using eq 6, since that expression is only valid for high  $\kappa a$  values.

As can be seen, the total average ion concentration inside the Stern layer generally exceeds the concentration of ions in the adjacent electrolyte solution. This is particularly true for low surface potentials when a strong ion adsorption is required to achieve a high anomalous surface conductivity. For  $pK = 2$ , the Stern layer is saturated at practically all  $y^0(a)$  values, while for lower  $pK$  values, the saturation condition requires increasingly higher surface potentials. It should be noted that the average ion concentration inside the Stern layer becomes lower than that of the adjacent solution for  $pK = -1$  and low  $y^0(a)$ . Actually, these two magnitudes become equal for low surface potential values when the second factor in the right-hand side

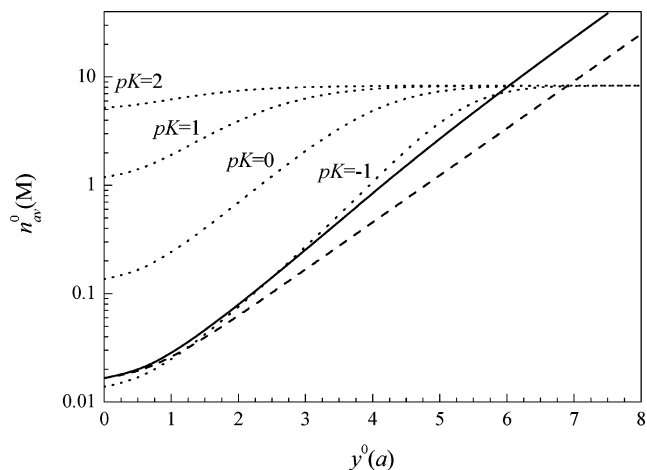


**Figure 1.** Total average ion density inside the Stern layer according to the M–W model (eqs 3–5) calculated for  $\kappa a = 30$  and the indicated  $pK$  values (dotted lines). The dashed line represents the total ion density in the diffuse layer at  $r = a$  (eq 4), while the solid line corresponds to the total average ion density inside the surface layer according to our model.

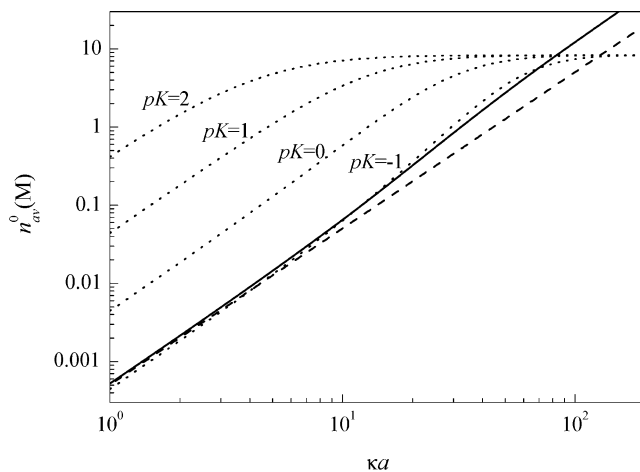


**Figure 2.** Same as Figure 1, but calculated for the nondimensional surface potential  $y^0(a) = 4$ .

of eq 5 becomes equal to  $z_j e h$ , that is when  $pK \approx -0.9$  (for  $eN_j = 80 \mu\text{C cm}^{-2}$ ).

For high, but still reasonable, surface potential values,  $y^0(a) > 6$  (for  $eN_j = 80 \mu\text{C cm}^{-2}$ ), the Stern layer becomes fully saturated for any value of  $pK$ , while the ion density in the diffuse layer continues to increase. This saturation can be regarded as a positive feature of the M–W model of the Stern layer, since it avoids excessively high ion concentrations that are obtained in the framework of the standard model due to the assumption that ions can be treated as mathematical points. However, the M–W model includes both the inner and the outer regions, and no measures are taken in order to avoid excessive ion concentrations in the outer region. Therefore, all the reservations about the applicability of the standard model at high surface potential values also apply to the M–W model.

Figures 1 and 2 provide a means to compare the anomalous surface conductivity with the surface conductivity of the diffuse double layer, since both values are proportional to the corresponding ion densities. However, it is worth noting that the proportionality constants are different, mainly because the thickness of the surface layer is fixed while that of the diffuse layer depends on the electrolyte concentration: the Debye length in Figure 2 varies in the range 100 to 0.5 times the thickness  $h$  of the surface layer. Another important reason is that the fluid

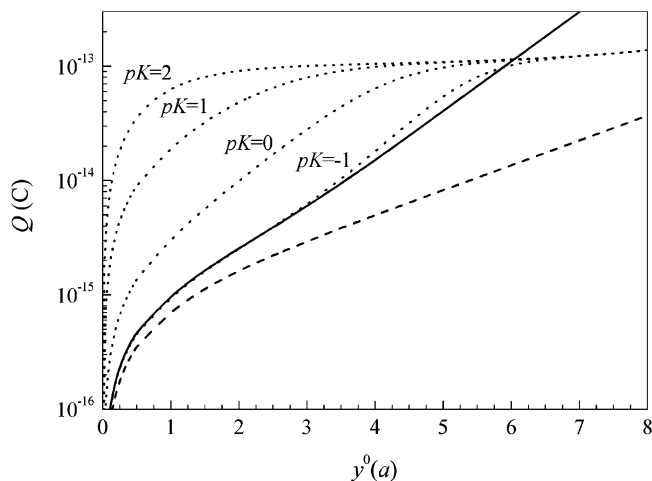


**Figure 3.** Total fixed charge on the surface of the core according to the M–W model, calculated for  $\kappa a = 30$  and the indicated  $pK$  values (dotted lines). The dashed line represents the total fixed charge according to the bare particle model, while the solid line corresponds to the total fixed charge inside the surface layer according to our model.

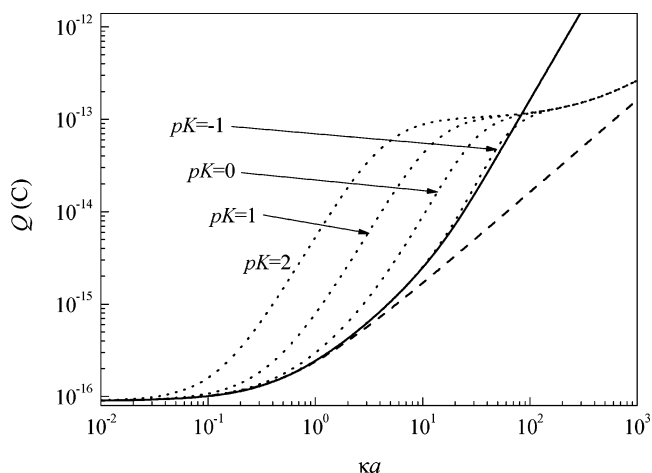


**Figure 4.** Same as Figure 3, but calculated for the dimensionless surface potential  $y^0(a) = 4$ .

does not move inside the surface layer according to the M–W model, while it does move in the diffuse layer, enhancing its surface conductivity value. Finally, the diffusion coefficient values for ions inside the surface layer need not be equal to those in the bulk solution (we do not consider this possibility in the present work).

As a final comment, it is important to note that, while the M–W model specifies a mechanism for the dependence of the Stern layer properties on the system parameters, it does not specify any mechanism that determines the value of the fixed surface charge on the core of the particle. However, this charge has an extremely strong dependence on  $y^0(a)$  and  $\kappa a$ , as shown in Figures 3 and 4, which were obtained using the same choice of parameters as Figures 1 and 2, respectively. As can be seen, for low surface potentials and intermediate  $\kappa a$  values, the fixed surface charge can be nearly 2 orders of magnitude higher than in the bare particle model.

**2.2. Proposed Model.** Our model can be regarded as an extension of the M–W model. We also consider that the particle is made of a rigid core surrounded by a thin surface layer of thickness  $h \approx 10 \times 10^{-10}$  m. The radius of the whole system is  $a$ , and for  $r > a$ , the standard electrokinetic equations apply. Any differences with the M–W model correspond, therefore, to the region  $0 < x < h$ .

The first difference is that we consider the fixed charges of the particle to be distributed inside this region, rather than forming a surface charge layer precisely on the core surface:  $x = 0$ . This assumption implies that the core is not necessarily a perfectly smooth sphere, that the fixed charges have a finite size and need not be completely immersed inside the core, and that a hairy surface is a possible reality.<sup>17,18</sup>

The second difference is that we do not require a priori that the fluid cannot move inside the surface layer. This requirement is necessary in any treatment of the surface layer in which it is assumed to be infinitely thin,<sup>4,5</sup> since, in this case, it is impossible to write down the Navier–Stokes equation. However, when the layer is assumed to have a finite thickness, as in the M–W and our models, this requirement is no longer necessary. Besides, if hydrated ions are allowed to move inside the surface layer, it seems reasonable that water molecules should also be allowed to move. While the use of macroscopic equations at length scales on the order of  $10 \times 10^{-10}$  m can certainly be objected, this is done in the M–W model just outside the hydrodynamic radius  $r = a$  (and in all the existing treatments that use the standard model). It is worth noting that, for a concentration  $n^\infty = 0.1$  M, a quite usual value, the Debye screening length is approximately  $10 \times 10^{-10}$  m.

The third difference is that we do not use any adsorption isotherm, at least in this initial formulation of the model. On the contrary, ions are free to move across the external boundary driven by the electric potential and concentration gradients, as well as the fluid flow. Since one of the boundary conditions at  $r = a$  is the continuity of the ion concentrations, the ion densities inside the surface layer are close to the densities just outside the layer: solid lines in Figures 1 and 2. Therefore, our model predicts lower ion densities at low surface potentials than the M–W model and higher in the opposite case. However, this does not mean that the resulting surface conductivity values are always weaker at low surface potentials, since the fluid flow inside the surface layer greatly enhances the anomalous surface conductivity. Furthermore, while the ion density in the diffuse layer is identical for the three considered models, the corresponding surface conductivity is higher according to our model because the adhesion boundary condition applies at  $r = a - h$  rather than  $r = a$ .

The fourth and final difference is in the value of the fixed charge. Just as in the M–W model, we do not specify any mechanism determining the value of this charge as a function of the system parameters, at least in this initial formulation of the model. However, the resulting values strongly differ from those of the M–W model, being generally lower and closer to the values corresponding to the bare particle model, at least for low surface potentials or low  $\kappa a$  values (solid lines in Figures 3 and 4).

In view of the assumptions specified above, the mathematical formulation of the proposed model is identical to that presented earlier for the description of the dielectric and electrokinetic properties of dilute suspensions of soft particles.<sup>24,25</sup> For this reason, we do not rewrite here any of the governing equations and boundary conditions that determine the predicted behavior of the system. We only note that the soft particle model includes a parameter  $\lambda$  related to the resistance exerted by the polymer segments in the permeable membrane to the fluid flow inside it according to the Debye–Bueche model.<sup>26</sup> In order to simplify the forthcoming discussion and to minimize the number of parameters, we only consider now the extreme case  $\lambda = 0$ : free fluid flow inside the surface layer. We furthermore assume that the diffusion coefficients of all the ionic species have the same

value inside the surface layer as in the bulk solution, and that the permittivity inside this layer is the same as in the bulk.

A simple estimate of a physically meaningful value of the parameter  $\lambda$  can be made, assuming that the drag exerted on the fluid flow by each fixed charge in the surface layer is the same as the force  $F$  exerted by the fluid on a moving ion in the suspending medium

$$F = \frac{v}{u} = \frac{vkT}{D}$$

where  $v$  is the ion velocity,  $u$  its mobility,  $D$  its diffusion coefficient, and the Einstein relation was used in order to write the second equality.

The drag coefficient in the soft particle model is defined as<sup>24</sup>

$$\lambda^2 = \frac{\gamma}{\eta}$$

where  $\gamma$  is the force per unit volume and unit velocity. Combining the above expressions gives

$$\lambda^2 = \frac{kT}{D\eta} \frac{Q/e}{4\pi a^2 h} \quad (8)$$

where  $Q$  is the fixed charge of the particle, so that the second factor in the right-hand side is the number of fixed ions per unit volume in the surface layer. The value of  $Q$  strongly depends on the surface potential and on  $\kappa a$ , increasing with these parameters (Figures 3 and 4). Therefore, the assumption  $\lambda = 0$  is acceptable for weakly charged particles in dilute electrolyte solutions but becomes objectionable in the opposite limit.

### 3. Results and Discussion

In what follows, we compare our results to those corresponding to bare particles (no surface layer) and to the results of the M–W model, keeping constant the equilibrium electric potential value at  $r = a$ . For the bare and the M–W models, this parameter coincides precisely with the  $\zeta$  potential. However, this is not exactly the case for our model, since as is well-known,<sup>27</sup> the  $\zeta$  potential is an ill-defined parameter in the case of soft particles (the standard definition is only possible for  $\lambda = 0$  or  $\lambda \rightarrow \infty$ , since in these cases, the  $\zeta$  potential would coincide with the equilibrium surface potential at  $r = a - h$  and  $r = a$ , respectively). Nevertheless, this fact is of little importance for the extremely thin membranes considered in this study. It should be noted that this representation differs from that used in ref 24, where the comparisons were made by keeping constant the fixed charge of the particle. The reason for the change is in the extremely high variability of the particle charge across the considered models as shown in Figures 3 and 4.

The different parameter values used in the calculations, except when specified otherwise, are given in Table 1.

Figure 5 represents the conductivity increment  $\Delta K$  defined as

$$K = K^\infty(1 + \phi\Delta K) = K^\infty(1 + 3\phi d) \quad (9)$$

and calculated as a function of the dimensionless surface potential for three values of  $\kappa a$ . In the above expression,  $K$  is the conductivity of the suspension,  $K^\infty$  the conductivity of the suspending medium,  $\phi$  the volume fraction of particles, and  $d$  the dipolar coefficient. For very low surface potential values, the bare particle behaves just as an insulating sphere so that its dipole coefficient has the value  $-1/2$ , irrespective of the value

**TABLE 1: Parameter Values Used in Figures 5–8, except When Specified Otherwise**

radius of the core and surface layer	$a = 100 \times 10^{-9}$ m
thickness of the surface layer	$h = 1 \times 10^{-9}$ m
absolute permittivity outside the core	$\epsilon = 78.55 \times 8.85 \times 10^{-12}$ F m <sup>-1</sup>
viscosity of the suspending medium	$\eta = 0.89 \times 10^{-3}$ poise
temperature	$T = 298$ K
number of ionic species in the solution	$N = 2$
ion valences	$z_1 = -z_2 = 1$
ion diffusion coefficients	$D_1 = D_2 = 2 \times 10^{-9}$ m <sup>2</sup> s <sup>-1</sup>
electrolyte concentration such that dimensionless surface potential	$\kappa a = 30$
M–W maximum Stern layer surface charge	$y^0(a) = 4$
M–W dissociation constant $pK$	$eN_1 = eN_2 = 80 \mu\text{C cm}^{-2}$ $pK_1 = pK_2 = 2$

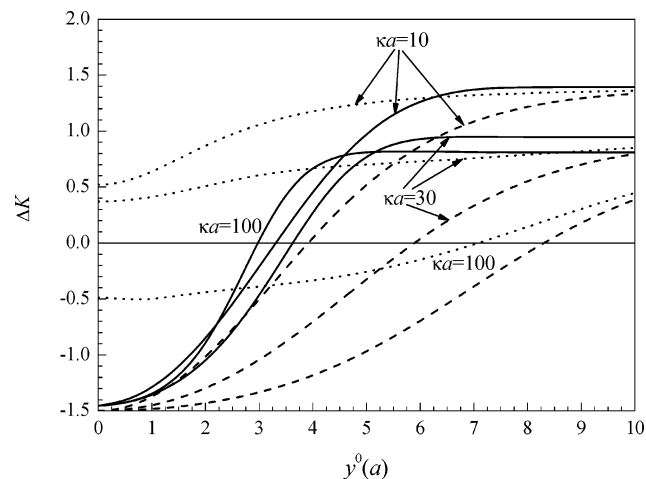


**Figure 5.** Conductivity increment defined in eq 9, calculated for the indicated  $\kappa a$  values. Dashed lines: bare particle model. Dotted lines: M–W model. Solid lines: our model.

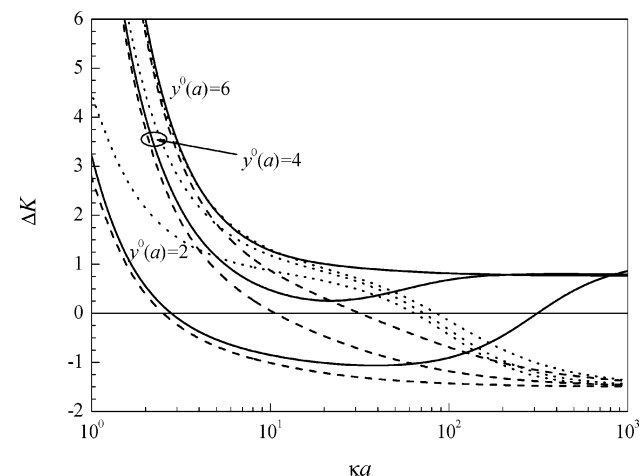


**Figure 6.** Same as Figure 5, but calculated for the indicated dimensionless surface potential values.

of  $\kappa a$ ,<sup>28</sup> and the corresponding conductivity increment curves tend toward  $-3/2$ . Our model tends toward a slightly higher value because the radius of the core ( $a - h$ ) is smaller than the radius ( $a$ ) of the bare particle. Therefore, the limiting conductivity increment value is  $-(3/2)[(a - h)/a]^3 \approx -1.45$ .

A totally different behavior is observed for the M–W model: the conductivity increment values are much higher and strongly depend on the electrolyte concentration, decreasing with

*ka*. The first feature is due to the presence of the adsorption isotherm (eq 1) that populates the Stern layer even for uncharged particles (Figure 1), leading to a nonvanishing surface conductivity. As for the dependence on *ka*, it arises because the static dipole coefficient of uncharged particles is determined by the simple expression<sup>28</sup>

$$d = \frac{2Du - 1}{2Du + 2}$$

where *Du* is the Dukhin number: total surface conductivity divided by the particle radius and the bulk conductivity. For uncharged particles, the dependence of *Du* on *ka* is determined by the denominator in eq 1, since the ion concentration in the numerator cancels with that in the expression of the bulk conductivity. Therefore, *Du* decreases with increasing *ka* and so does the dipolar coefficient.

For high  $y^0(a)$  values, the conductivity increment of bare particles also increases, basically due to an increment of the surface conductivity of the diffuse double layer, and tends to a finite value for  $y^0(a) \rightarrow \infty$  (in the simplest case of univalent electrolytes, equal diffusion coefficients values of counterions and co-ions, and  $\kappa a \rightarrow \infty$ , the theoretical limit of the dipolar coefficient is  $1/4$ ,<sup>29</sup> so that the conductivity increment tends to 0.75). The M–W and our models tend to the same limiting values as the bare particle model, since when the surface conductivity of the diffuse double layer diverges, the contribution of the inner layer becomes irrelevant.

For intermediate  $y^0(a)$  values, our model has a very strong dependence on the surface potential, due to the strong dependence of the ion density in the surface layer on this same parameter (Figure 1). As can be seen, the conductivity increment is always substantially greater than for bare particles, as expected in view of the additional surface conductivity of the surface layer and the increased surface conductivity of the diffuse layer. A comparison with results deduced using the M–W model shows that for low surface potential values  $\Delta K$  is lower according to our model, at least for the adsorption isotherm parameters used in Figure 5, because of the lower ion density values in the surface layer (Figure 1). However, for high  $y^0(a)$ , our conductivity increment surpasses the values obtained by the M–W model, since the ion density inside the surface layer increases (Figure 1), while the fluid flow inside this layer enhances the surface conductivity.

Figure 6 represents the conductivity increment calculated as a function of *ka* for three values of the surface potential. For low electrolyte concentrations, the bare particle model leads to very large conductivity increment values that are mainly caused by the increment of the effective size of the particles due to their thick diffuse double layer.<sup>29</sup> In the opposite high concentration limit, the surface conductivity increases with the square root of the electrolyte concentration (eqs 6 and 7), while the bulk conductivity is proportional to this concentration, so that the Dukhin number becomes vanishingly small and the conductivity increment tends to  $-3/2$ , irrespective of the surface potential value.<sup>29</sup>

The behavior of the M–W model is qualitatively similar to that of the bare particle model, leading always to higher conductivity increment values due to the additional Stern layer surface conductivity term. At low *ka*, the differences are very small, except for low surface potentials when the surface conductivity of the diffuse double layer decreases and the contribution to the dipole coefficient of the Stern layer becomes increasingly important (Figure 5). The differences are highest at intermediate concentrations when the Stern layer surface

conductivity term becomes dominant. Finally, for the high *ka* limit, the Stern layer surface conductivity attains its saturation value (Figure 2), so that Dukhin number tends to zero just as for the bare particle model.

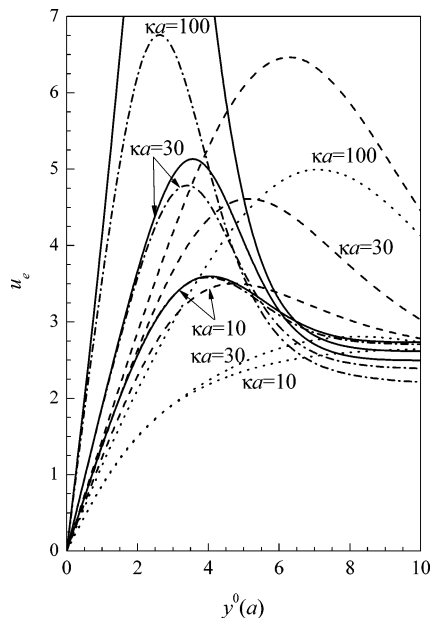
As for our model, it also leads always to higher conductivity increment values than the bare particle model, due to the additional surface conductivity of the surface layer and the increased surface conductivity of the diffuse layer. At low ion concentrations, the differences are always very small, because the contribution of the surface layer becomes negligible as compared to the diffuse double layer: for decreasing *ka*, its thickness remains fixed, while the Debye screening length increases. Due to this same reason, the surface conductivity of the diffuse layer tends to that of the bare particle model. At intermediate *ka* values, the differences become quite important especially for high surface potential values, when the inner layer conductivity can surpass that of the M–W model. Finally, in the high concentration limit, our model leads to conductivity increment values that are positive and much higher than the other two models. The reason for this behavior is that the average ion density in the surface layer is proportional to the ion concentration at  $r = a$ , which is proportional to the bulk ion concentration (eq 4 and Figure 2). Therefore, the surface layer conductivity increases linearly with the electrolyte concentration so that, for high *ka* values, the Dukhin number tends to a constant value rather than decreasing to zero as for the other two models.

Figure 7 represents the dimensionless electrophoretic mobility

$$u_e = \frac{3e\eta}{2\epsilon\kappa_B T} \frac{v_e}{E} \quad (10)$$

calculated as a function of the dimensionless surface potential for three different values of the product *ka*. In this expression,  $v_e$  is the electrophoretic velocity and *E* is the applied electric field. The three bare particle model curves reflect the well-known behavior:<sup>30</sup> an initial increase corresponding to an increasing surface charge in the diffuse double layer, a maximum value (present for sufficiently high *ka*), and a decrease due to the increment of the dipolar coefficient and a corresponding decrement of the total tangential electric field value in the diffuse double layer. The final limiting value is determined by the corresponding limit of the dipolar coefficient (Figure 5 and eq 9).

As can be seen, the anomalous surface conductivity can have a tremendous impact on the electrophoretic mobility value. The most important qualitative conclusion drawn from Figure 7 is that, according to our model, the mobility generally increases with the surface conductivity, while it always decreases according to the M–W model. The reason for the behavior of the M–W model is rather obvious: the diffuse layer and the fluid boundary condition are the same as in the bare particle model, while the tangential electric field is lower because the dipole coefficient is always higher (Figure 5 and eq 9). As for our model, the mobility at low surface potentials is sensibly higher than for the bare particle model, because the slipping plane is shifted to  $r = a - h$  so that all the ions in the diffuse double layer and an important fraction of free ions in the surface layer are located relatively far from the slipping plane, which increases the tangential fluid velocity along the surface of the particle. For higher surface potential values, this difference decreases and even changes sign due to the faster increase of the dipole coefficient in our model (Figure 5). Finally, Figure 7 also illustrates the influence of the  $\lambda$  parameter value,



**Figure 7.** Dimensionless electrophoretic mobility defined in eq 10, calculated for the indicated  $\kappa a$  values. Dashed lines: bare particle model. Dotted lines: M–W model. Solid lines: our model. Dot and dash lines: our model with the parameter  $\lambda$  value estimated using eq 8.

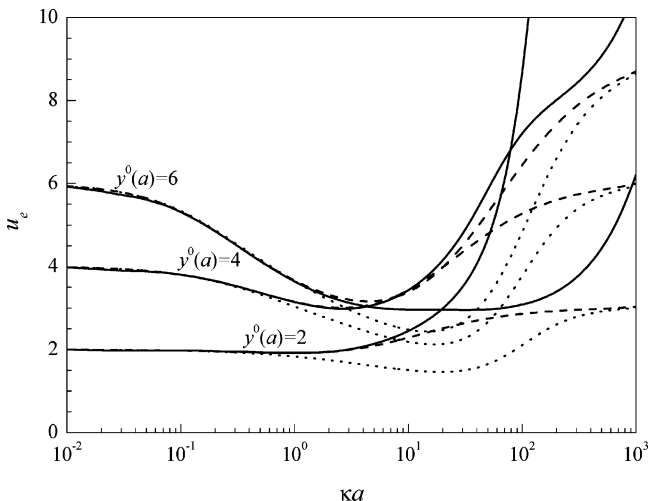


**Figure 8.** Same as Figure 7, but calculated for the indicated dimensionless surface potential values and for  $\lambda = 0$  only.

calculated using eq 8, on the electrophoretic mobility. As can be seen, the mobility values are always lowered with respect to the values obtained considering that  $\lambda = 0$ , the difference being important for  $\kappa a = 100$  but negligible for  $\kappa a = 10$ .

Figure 8 shows the dependence of the electrophoretic mobility on  $\kappa a$ , calculated for three different values of the surface potential. The bare particle model shows the well-known behavior:<sup>31</sup> Debye–Hückel limit for low  $\kappa a$  and Smoluchowski value in the opposite limit. The M–W model displays these same limiting behaviors, because the anomalous surface conductivity vanishes at low  $\kappa a$  (eq 1), while the dipole coefficient value coincides with that of the bare particle model at high  $\kappa a$  (Figure 6). For intermediate electrolyte concentrations, the mobility is always lowered due to the higher dipole coefficient values (Figure 5).

As for our model, it also tends to the Debye–Hückel limit at low electrolyte concentrations, because the surface layer conductivity vanishes under these conditions (Figure 2), while the surface conductivity of the diffuse layer tends to that of the

bare particle model. For intermediate  $\kappa a$  values and moderate surface potential, the mobility becomes much higher than in the bare particle model, because an important fraction of free charges is located far from the zero fluid velocity boundary. However, the mobility becomes lower for high  $y^0(a)$ , in view of the high value of the dipole coefficient (Figure 5). In order to provide an interpretation of the strong increase of the mobility for the high  $\kappa a$  limit, we solve the Navier–Stokes equation in one dimension inside the surface layer and the electrolyte solution considering, as in all of this work, that there is no resistance exerted by the fixed charges in the surface layer to the fluid flow

$$\eta \frac{d^2 v_y}{dx^2} = \rho E_y$$

In this expression,  $x$  is the radial coordinate extending from the core ( $x = 0$ ) and into the electrolyte solution ( $x > h$ ),  $v_y = v_y(x)$  is the tangential fluid velocity,  $\rho = \rho(x)$  is the free ion charge,  $E_y$  is the tangential electric field, and the pressure term has been omitted in view of symmetry considerations. This equation can be combined with the equilibrium Poisson equation

$$\frac{d^2 \Psi^0}{dx^2} = -\frac{\rho + \rho^f}{\epsilon}$$

where  $\rho^f$  is the density of fixed charges inside the layer, leading to

$$\eta \frac{d^2 v_y}{dx^2} = -\epsilon \frac{d^2 \Psi^0}{dx^2} E_y - \rho^f E_y$$

The solution of this equation inside the surface layer is

$$\eta v_y = -\epsilon \Psi^0 E_y - \rho^f E_y x^2/2 + K_1 x + K_0$$

while, outside it, it reduces to

$$\eta v_y = -\epsilon \Psi^0 E_y + C_1 x + C_0$$

The four unknown coefficients can be determined using the following boundary conditions:

1. For  $x \rightarrow \infty$ , the electric potential vanishes, while the fluid velocity attains a finite value

$$C_1 = 0$$

$$C_0 = \eta v_y(\infty)$$

2. For  $x = 0$ , the fluid velocity vanishes, while the electric potential attains a finite value

$$K_0 = \epsilon \Psi^0(0) E_y$$

3. For  $x = h$ , the electric potential is continuous, and the velocity is continuous, as is its first derivative with respect to  $x$ .<sup>24</sup> Finally, the first derivative of the potential is also continuous, because  $\epsilon$  is continuous and there is no surface charge density

$$K_1 = \rho^f h E_y$$

Therefore, the fluid velocity value far from the surface layer is

$$\eta v_y(\infty) = \epsilon \Psi^0(0) E_y + \rho^f E_y h^2/2$$

For the limit  $h \rightarrow 0$ , this result reduces to the well-known expression

$$\eta v_y(\infty) = \epsilon \Psi^0(0) E_y$$

In the case that  $\kappa a \rightarrow \infty$  while the fixed charge density is kept at a constant value, the potential  $\Psi^0(0) \rightarrow 0$ , so that our result reduces to

$$\eta v_y(\infty) = \rho^f E_y h^2 / 2$$

which coincides with the result presented in ref 24. In the general case and for high  $\kappa a$  values while keeping constant the surface potential,  $\Psi^0(0)$  remains approximately constant with a value close to and slightly higher than  $\Psi^0(h)$ . On the contrary, the fixed charge diverges with diverging  $\kappa a$  (Figure 4), so that the electrophoretic mobility (eq 10) also diverges.

### Conclusion

We presented a new generalization of the standard electrokinetic model, often used for the interpretation of the dielectric and electrokinetic properties of aqueous colloidal suspensions. Since our model can be regarded as being based on the existing model of Mangelsdorf and White, at this first stage we only discussed its simplest features in order to visualize its potential. This is why we considered that fluid flow is unrestricted inside the surface layer ( $\lambda = 0$ ) and that there is no specific adsorption of ions onto that layer.

It should be stressed that these assumptions are not part of our model. On the contrary, the parameter  $\lambda$  can be freely assigned any value  $0 \leq \lambda < \infty$  and, for  $\lambda \rightarrow \infty$ , the fluid ceases to flow inside the surface layer just as in the M–W model. A simple estimate of the parameter  $\lambda$  (eq 8) shows that the assumption  $\lambda = 0$  is reasonable for weakly charged particles in dilute electrolyte solutions but becomes objectionable in the opposite limit. As for the specific adsorption, it can be easily incorporated into the model by considering that the equilibrium concentrations of ions inside the surface layer are determined in a way similar to that used in ref 32. With these two additions, our model can be made to behave just as the M–W model. However, the trends outlined in the present paper show that it could be used for the interpretation of a broader set of experimental data, including those cases when the measured mobility is higher than predicted by the standard model.

In a future work, we intend to include these generalizations and present the solution of our model in the frequency domain in order to analyze its potential for the interpretation of electrokinetic and dielectric spectroscopy data.

**Acknowledgment.** Financial support for this work by MEC (project FIS2006-4460), FEDER funds, and Junta de Andalucía (project FQM-410), of Spain; and CIUNT (project 26/E312)

and CONICET (project PIP 6456), of Argentina, is gratefully acknowledged.

### References and Notes

- (1) O'Brien, R. W.; Perrins, W. T. *J. Colloid Interface Sci.* **1984**, *99*, 20.
- (2) Zukoski, C. F.; Saville, D. A. *J. Colloid Interface Sci.* **1985**, *107*, 322.
- (3) Kijlstra, J.; Van Leeuwen, H. P.; Lyklema, J. *Langmuir* **1993**, *9*, 1625.
- (4) Simonova, T. S.; Shilov, V. N. *Kolloidn. Zh.* **1986**, *48*, 370.
- (5) Zukoski, C. F.; Saville, D. A. *J. Colloid Interface Sci.* **1986**, *114*, 32.
- (6) Mangelsdorf, C. S.; White, L. R. *J. Chem. Soc., Faraday Trans.* **1990**, *86*, 2859.
- (7) Zukoski, C. F.; Saville, D. A. *J. Colloid Interface Sci.* **1986**, *114*, 45.
- (8) Arroyo, F. J.; Carrique, F.; Delgado, A. V. *J. Colloid Interface Sci.* **1999**, *217*, 411.
- (9) Rosen, L. A.; Baygents, J. C.; Saville, D. A. *J. Chem. Phys.* **1993**, *98*, 4183.
- (10) Mangelsdorf, C. S.; White, L. R. *J. Chem. Soc., Faraday Trans.* **1998**, *94*, 2441.
- (11) Mangelsdorf, C. S.; White, L. R. *J. Chem. Soc., Faraday Trans.* **1998**, *94*, 2583.
- (12) Dunstan, D. E. *J. Colloid Interface Sci.* **1994**, *163*, 255.
- (13) Myers, D. F.; Saville, D. A. *J. Colloid Interface Sci.* **1989**, *131*, 461.
- (14) Rosen, L. A.; Saville, D. A. *Langmuir* **1991**, *7*, 36.
- (15) Rosen, L. A.; Saville, D. A. *J. Colloid Interface Sci.* **1990**, *140*, 82.
- (16) Rosen, L. A.; Saville, D. A. *J. Colloid Interface Sci.* **1992**, *149*, 542.
- (17) Van der Put, A. G.; Bijsterbosh, B. H. *J. Colloid Interface Sci.* **1983**, *92*, 499.
- (18) Elimalech, M.; O'Melia, C. *Colloids Surf.* **1990**, *44*, 165.
- (19) Kleijn, J. M. *Colloids Surf.* **1990**, *51*, 371.
- (20) Raziilov, I. A.; Zharkikh, N. I.; Dukhin, S. S. *Colloid J.* **1995**, *57*, 678.
- (21) Raziilov, I. A.; Zharkikh, N. I.; Gonzalez-Caballero, F.; Delgado, A. V.; Dukhin, S. S. *Colloids Surf.* **1997**, *121*, 173.
- (22) Born, M. Z. *Phys.* **1920**, *1*, 45.
- (23) Dukhin, S. S.; Shilov, V. N. *Dielectric Phenomena and the Double Layer in Disperse Systems and Polyelectrolytes*; Wiley: New York, 1974.
- (24) López-García, J. J.; Grosse, C.; Horno, J. J. *Colloid Interface Sci.* **2003**, *265*, 327.
- (25) López-García, J. J.; Grosse, C.; Horno, J. J. *Colloid Interface Sci.* **2003**, *265*, 341.
- (26) Debye, P.; Bueche, A. *J. Chem. Phys.* **1948**, *16*, 573.
- (27) Ohshima, H. In *Encyclopedia of Surface and Colloid Science*; Hubbard, A. T., Ed.; Dekker: New York, 2002; Vol 2.
- (28) Grosse, C.; Barchini, R. *J. Phys. D* **1992**, *25*, 508.
- (29) Grosse, C.; Pedrosa, S.; Shilov, V. N. *J. Colloid Interface Sci.* **2002**, *251*, 304.
- (30) O'Brien, R. W.; White, L. R. *J. Chem. Soc., Faraday Trans. 2* **1978**, *74*, 1607.
- (31) Wiersema, P. H.; Loeb, A. L.; Overbeek, J. Th. G. *J. Colloid Interface Sci.* **1966**, *22*, 70.
- (32) López-García, J. J.; Grosse, C.; Horno, J. J. *Colloid Interface Sci.* **2002**, *254*, 287.